Inorg. Chem. **2002**, *41*, 1707–1716

Enhanced Selectivity for Actinides over Lanthanides with CMPO Ligands Secured to a C_3-Symmetric Triphenoxymethane Platform

Matthew W. Peters, Eric J. Werner, and Michael J. Scott*

Department of Chemistry, University of Florida, P.O. Box 117200, Gainesville, Florida 32611-7200

Received November 8, 2001

A ligand system containing three preorganized carbamoylmethylphosphine oxide (CMPO) moieties anchored onto a rigid C_3-symmetric triphenoxymethane platform has been developed for facile metal complexation and subsequent extraction from aqueous acidic nuclear waste streams. Intended to mimic the 3:1 CMPO–actinide stoichiometry of the extracted species in the TRUEX nuclear waste treatment process, the CMPO arms on this ligand are oriented such that all three CMPO moieties can cooperatively bind a metal ion. Extractions of simulated nuclear waste streams (10^{-4} M metal in 1 M nitric acid) with solutions of this ligand in methylene chloride (10^{-3} M) reveal a high affinity for the actinide thorium and a very low, but constant, affinity for the lanthanides across the series. Thorium and five lanthanide (lanthanum, cerium, neodymium, europium, and ytterbium) nitrate complexes of this ligand have been synthesized and fully characterized by X-ray crystallography, ^{1}H and ^{31}P NMR spectra, and FT-ICR-MS to elucidate the mechanism of this unique actinide selectivity. All six oxygen donors from the three CMPO arms of the ligand and one or two nitrate counterions coordinate these metals to afford 2+ cationic complexes in every case. Because of the large size of the ligand, both the thorium and lanthanide complexes present similarly charged and sized surfaces to the extraction solvents, but the thorium complex is extracted quantitatively over the lanthanide complexes. A possible rationale for this extraction behavior difference is presented and further illustrated by the extraction properties of this ligand system for the alkali metals (lithium, sodium, potassium, rubidium, and cesium) as picrate salts and by the solid- and solution-state structures of its lithium picrate complex.

Introduction

The processing of acidic actinide solutions such as those found in typical nuclear waste streams requires the separation of actinide radionuclides from the chemically similar but relatively innocuous lanthanides. To fulfill this need, several actinide/lanthanide separation strategies have been developed, and of these, liquid−liquid extractions with carbamoylmethylphosphine oxide (CMPO) based ligands have been one of the most widely used and studied.[1,2] In particular, the ability of octyl(phenyl)(*N*,*N*-diisobutylcarbamoylmethyl)-phosphine oxide, **1**, to remove actinides from nitric acid solutions of fission products via metal coordination with its carbonyl and phosphoryl oxygen atoms and subsequently transfer these metals into an organic solvent medium has been exploited in the *tr*ans-*u*ranium *ex*traction (TRUEX) process.[2] Although this method can readily sequester actinides, lanthanides are still extracted in quantities that complicate processing. Along with advancing traditional nuclear waste processing, an improvement of the efficiency of an actinide/lanthanide separation protocol will increase the feasibility of the currently impractical transmutation of long-lived ($t_{1/2} \sim 10^3$−10^4 years) actinide isotopes into short-lived ($t_{1/2} \sim 10^1$ years) and more practically stored lanthanides. Without their removal, the daughter lanthanide products produced by the neutron bombardment of actinides (the mechanism of transmutation) absorb these neutrons, shielding the remaining actinides.[3]

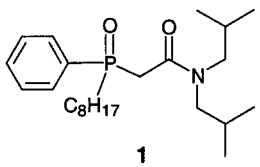

1

* To whom correspondence should be addressed. Fax: 352-392-3255. E-mail: mjscott@chem.ufl.edu.

(1) Nash, K. L.; Choppin, G. R. *Sep. Sci. Technol.* **1997**, *32*, 255.
(2) (a) Horwitz, E. P.; Kalina, D. G.; Diamond, H.; Vandegrift, G. F.; Schulz, W. W. *Solvent Extr. Ion Exch.* **1985**, *3*, 15. (b) Schulz, W. W.; Horwitz, E. P. *Sep. Sci. Technol.* **1988**, *23*, 1191.

10.1021/ic011144x CCC: $22.00
Published on Web 03/14/2002

The CMPO−actinide complexes formed during the TRUEX extraction procedure have been extensively studied to develop ligand modifications and process changes that might increase its selectivity for actinides.[4−7] For example, a 3:1 CMPO to metal stoichiometry has been implicated for americium species extracted from the acidic aqueous phase into the organic phase during the TRUEX process.[7] Inspired by this fact, groups in the 1990s attached multiple CMPO moieties to a variety of calixarene and calixarene-like platforms and were able to extract actinides with these ligands at higher selectivities than seen in comparable experiments with mono-CMPO extractants.[8−12] The most extensively studied group of these ligand systems contained four CMPO moieties tethered to the narrow and wide rims of calix[4]arenes, **2** and **3**, and although an increase in actinide affinity relative to the mono-CMPO ligands was generally found, the lanthanide selectivity of these ligands proved to be less predictable. The affinity for lanthanides in these systems varied widely across the series, with the selectivity toward some lanthanides equaling that of the actinides.[10] Additionally, the multi-CMPO ligand systems presented in the literature have thus far lacked definitive characterizations of the ligand−metal complexes formed during the extraction experiments. Such a detailed understanding of the chemical basis for the metal selectivities of these ligands is essential for creating improved metal extracting systems. Inspired by these same TRUEX studies and the calix[4]arene work that followed, we have developed a tris-CMPO ligand system that mimics the 3:1 TRUEX stoichiometry and have demonstrated that it is selective in extraction experiments for actinides. An analysis of the thorium and lanthanide complexes of this ligand in relation to its metal extraction properties is detailed herein.

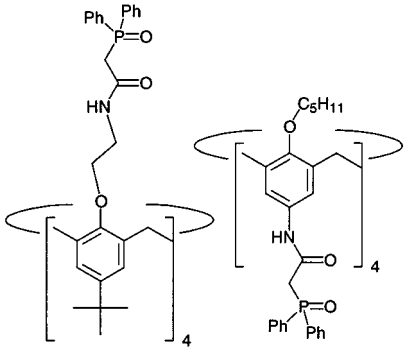

2 **3**

Experimental Section

General Considerations. The lanthanide and actinide salts, $La(NO_3)_3 \cdot 6H_2O$ (Alpha Aesar), $Ce(NO_3)_3 \cdot 6H_2O$ (Aldrich), $Nd(NO_3)_3 \cdot 6H_2O$ (Aldrich), $Eu(NO_3)_3 \cdot 5H_2O$ (Aldrich), $Yb(NO_3)_3 \cdot 5H_2O$ (Aldrich), $UO_2(NO_3)_2 \cdot 6H_2O$ (Strem), and $Th(NO_3)_4 \cdot 4H_2O$ (Strem), were used as received. The solutions were prepared from 18 MΩ Millipore deionized water, TraceMetal grade HNO_3 (Fisher Scientific), and freshly distilled organic solvents. The salts, Li picrate, Na picrate, K picrate, Rb picrate, and Cs picrate, were synthesized using 0.1 M picric acid (Aldrich) as described previously.[13,14] A Varian Cary 50 UV/vis spectrophotometer was used for the Arsenazo(III) and picrate assays. ICP-MS measurements were made by ALS Chemex in North Vancouver, BC, Canada. Elemental analyses were performed by Complete Analysis Laboratories, Inc. in Parsippany, NJ. All ^1H, ^{13}C, and ^{31}P NMR spectra were recorded on a Varian VXR-300 or Mercury-300 spectrometer at 299.95, 75.4, and 121.42 MHz for the proton, carbon, and phosphorus channels, respectively. IR spectra were recorded as KBr disks on a Bruker Vector-22 instrument at a resolution of 2 cm^{-1}. Mass spectrometry samples were analyzed on a Bruker Apex II 4.7T Fourier transform ion cyclotron resonance mass spectrometer (Bruker Daltonics, Billerica, MA). The MS analysis was by nanoelectrospray in positive ion mode with side-kick trapping and broad-band excitation from 300 to 5000 *m*/*z*. The MS samples were prepared at approximately 10 μM levels in methanol with 1% nitric acid and sprayed from 5 μm tapered Pico-Tips (New Objective, Cambridge, MA) at 1200 V. Tris(3,5-*tert*-butyl-2-hydroxyphenyl)methane, **4**,[15] and *p*-nitrophenyl (diphenylphosphoryl)acetate, **7**,[8] were prepared as previously described. The synthetic methodology for the preparation of **8** has been adapted from procedures developed in work with phenols and calix[*n*]arene platforms.[8]

Lanthanide and Actinide Extractions. Following a modification of an extraction method and assay previously described,[10] 10^{-4} M solutions of La^{3+}, Ce^{3+}, Nd^{3+}, Eu^{3+}, Yb^{3+}, and Th^{4+} in 1 M nitric acid and a 10^{-3} M solution of **8** in methylene chloride were prepared. Into 20 mL scintillation vials were transferred 5 mL of a metal solution and 5 mL of the **8** solution using an Eppendorf micropipet. The vials were capped and placed into an orbital shaker for 15 h at 20 °C. The layers were allowed to fully separate. A 1 mL aliquot of each aqueous layer and 2.5 mL of 6.4×10^{-4} M Arsenazo(III) solution in sodium formate−formic acid buffer (pH = 2.8) were transferred to a 25 mL volumetric flask, and the flask

(3) Proceedings of the 5th OECD/NEA Information Exchange Meeting on Actinide and Fission Product Partitioning and Transmutation, Mol, Belgium, 1998, EUR 188898EN.
(4) (a) Horwitz, E. P.; Muscatello, A. C.; Kalina, D. G.; Kaplan, L. *Sep. Sci. Technol.* **1981**, *16*, 417. (b) Kalina, D. G.; Horwitz, E. P.; Kaplan, L.; Muscatello, A. C. *Sep. Sci. Technol.* **1981**, *16*, 1127. (c) Kalina, D. G.; Mason, G. W.; Horwitz, E. P. *J. Inorg. Nucl. Chem.* **1981**, *43*, 579. (d) Horwitz, E. P.; Kalina, D. G.; Kaplan, L.; Mason, G. W.; Diamond, H. *Sep. Sci. Technol.* **1982**, *17*, 1261. (e) Schulz, W. W.; Horwitz, E. P. *J. Less-Common Met.* **1986**, *122*, 125. (f) Chiarizia, R.; Horwitz, E. P. *Inorg. Chim. Acta* **1987**, *140*, 261.
(5) (a) Siddall, T. H. *J. Inorg. Nucl. Chem.* **1963**, *25*, 883. (b) Siddall, T. H. *J. Inorg. Nucl. Chem.* **1964**, *26*, 1991. (c) Stewart, W. E.; Siddall, T. H. *J. Inorg. Nucl. Chem.* **1968**, *30*, 3281. (d) Stewart, W. E.; Siddall, T. H. *J. Inorg. Nucl. Chem.* **1970**, *32*, 3599.
(6) (a) Caudle, L. J.; Duesler, E. N.; Paine, R. T. *Inorg. Chem.* **1985**, *24*, 4441. (b) Caudle, L. J.; Duesler, E. N.; Paine, R. T. *Inorg. Chim. Acta* **1985**, *110*, 91.
(7) (a) Horwitz, E. P.; Martin, K. A.; Diamond, H.; Kaplan, L. *Solvent Extr. Ion Exch.* **1986**, *4*, 449. (b) Horwitz, E. P.; Diamond, H.; Martin, K. A.; Chiarizia, R. *Solvent Extr. Ion Exch.* **1987**, *5*, 419.
(8) Arnaud-Neu, F.; Böhmer, V.; Dozol, J.; Grüttner, C.; Jakobi, R. A.; Kraft, D.; Mauprivez, O.; Rouquette, H.; Schwing-Weill, M.; Simon, N.; Vogt, W. *J. Chem. Soc., Perkin Trans. 2* **1996**, 1175.
(9) Matthews, S. E.; Saadioui, M.; Böhmer, V.; Barboso, S.; Arnaud-Neu, F.; Schwing-Weill, M.; Carrera, A. G.; Dozol, J. *J. Prakt. Chem./Chem.-Ztg.* **1999**, *341*, 264.
(10) Barboso, S.; Carrera, A. G.; Matthews, S. E.; Arnaud-Neu, F.; Böhmer, V.; Dozol, J.; Rouquette, H.; Schwing-Weill, M. *J. Chem. Soc., Perkin Trans. 2* **1999**, 719.
(11) Delmau, L. H.; Simon, N.; Schwing-Weill, M.; Arnaud-Neu, F.; Dozol, J.; Eymard, S.; Tournois, B.; Grüttner, C.; Musigmann, C.; Tunayar, A.; Böhmer, V. *Sep. Sci. Technol.* **1999**, *34*, 863.
(12) Arduini, A.; Böhmer, V.; Delmau, L.; Desreux, J.; Dozol, J.; Carrera, M. A. G.; Lambert, B.; Musigmann, C.; Pochini, A.; Shivanyuk, A.; Ugozzoli, F. *Chem. Eur. J.* **2000**, *6*, 2135.
(13) Moore, S. S.; Tarnowski, T. L.; Newcomb, M.; Cram, D. J. *J. Am. Chem. Soc.* **1977**, *99*, 6398.
(14) Koenig, K. E.; Lein, G. M.; Stuckler, P.; Kaneda, T.; Cram, D. J. *J. Am. Chem. Soc.* **1979**, *101*, 3553.
(15) Dinger, M. B.; Scott, M. J. *Eur. J. Org. Chem.* **2000**, 2467.

was filled to the mark with formate buffer. The metal concentrations of the aqueous phases were determined by measuring the absorbance of the sample using 665 nm for the actinide solutions and 655 nm for the lanthanide solutions. The extractability of each metal by the ligand was calculated using the formula % $E = 100\%(A_1 - A)/(A_1 - A_0)$, where A is the absorbance of the extracted aqueous phase with the Arsenazo(III) indicator, A_1 is the absorbance of the aqueous phase before extraction with the indicator, and A_0 is the absorbance of metal-free 1 M nitric acid and the indicator. The errors reported are based on the accuracy of the spectrophotometer or one standard deviation from the mean of 3 measurements, whichever was higher.

Alkali-Metal Extractions. *Warning*! *Picrate salts are potentially explosive and should be handled with great care*. Following a literature procedure,[13,14] 0.014 M Li and Na picrate, 0.015 M K picrate, and 0.010 M Rb and Cs picrate aqueous solutions were prepared. Aliquots of each picrate solution were transferred to 3 mL shell vials—1.10 mL Li and Na picrate, 1.00 mL K picrate, and 1.50 mL Rb and Cs picrate—using an Eppendorf micropipet. To each of these vials, 1.00 mL of 0.015 M **8** in $CHCl_3$ and enough $CHCl_3$ to dilute the concentration of **8** to match the aqueous layer concentration was added. The vials were capped and shaken for 5 min and then allowed to separate. From each vial, a 0.125 mL aliquot of the organic phase was carefully removed with a micropipet and added to a 25 mL volumetric flask, which was then filled to the mark with acetonitrile. The absorbances of the diluted samples were measured at 380 nm. The extractability of each picrate salt by **8** was calculated using the formula $\%E = 100\%(A_1 - A)/(A_1 - A_0)$, where A is the absorbance of the diluted extracted aqueous phase, A_1 is the absorbance of the diluted aqueous phase before extraction, and A_0 is the absorbance of acetonitrile. The errors reported are based on the accuracy of the spectrophotometer or one standard deviation from the mean of 3 measurements, whichever was higher.

Preparation of Tris(3,5-di-*tert*-butyl-2-(cyanomethoxy)phenyl)methane, 5. A 12.19 g portion (19.4 mmol) of **4** was dissolved in dry acetone (200 mL) with 26.81 g (194.0 mmol) of potassium carbonate, 29.08 g (194.0 mmol) of sodium iodide, and 9.80 g (155.0 mmol) of chloroacetonitrile, and the solution was refluxed 48 h under nitrogen. After the solvent was removed in vacuo, the product was taken up in ether, dried with $MgSO_4$, and filtered, and the solvent was removed. Recrystallization of the reddish brown crude material from ethanol afforded 11.04 g (75%) of colorless crystals. ^{1}H NMR ($CDCl_3$): $\delta = 1.22$ (s, 27 H; Ar−C(C*H*$_3$)$_3$), 1.40 (s, 27 H; Ar−C(C*H*$_3$)$_3$), 4.22 (s, 6H; Ar−O−C*H*$_2$CN), 6.22(s, 1 H; C−*H*), 7.24 (d, ^4J(H,H) = 2.4 Hz, 3H; Ar *H*), 7.29 (d, ^4J(H,H) = 2.4 Hz, 3H; Ar *H*). ^{13}C NMR ($CDCl_3$): $\delta = 151.4$ (Ar), 147.5 (Ar), 143.2 (Ar), 135.5 (Ar), 126.9 (Ar), 123.7 (Ar), 114.7 (*C*N), 57.6 (Ar−O−*C*H$_2$), 37.6 (*C*−H), 35.6 (Ar−*C*(CH$_3$)$_3$), 35.6 (Ar−*C*(CH$_3$)$_3$), 34.7 (Ar−O−CH$_2$*C*H$_2$), 31.3 (Ar−C(*C*H$_3$)$_3$, 31.2 (Ar−C(*C*H$_3$)$_3$). Anal. Calcd for $C_{49}H_{67}N_3O_3$: C, 78.88; H, 9.05; N, 5.63. Found: C, 78.69; H, 9.27; N, 5.67. Slow evaporation of a chloroform solution of the product afforded crystals suitable for structural analysis.

Preparation of Tris(3,5-di-*tert*-butyl-2-(2-aminoethoxy)phenyl)methane, 6. A diethyl ether solution of **5** (11.04 g, 15.0 mmol) was added dropwise over 30 min to a slurry of lithium aluminum hydride (7.60 g, 225.0 mmol) in diethyl ether at 0 °C. The mixture was allowed to warm to room temperature and stirred for an additional 12−15 h. A 10 mL portion of 5% NaOH was slowly added to the slurry, and the solution was allowed to stir for 30 min. The solution was dried with $MgSO_4$ and filtered, and the solvent was removed in in vacuo. The crude white solid was recrystallized from acetonitrile to give 10.41 g (91%) of product. ^{1}H NMR ($CDCl_3$): $\delta = 1.20$ (s, 27 H; Ar−C(C*H*$_3$)$_3$), 1.34 (s, 27 H; Ar−C(C*H*$_3$)$_3$) 2.01 (b, 6H; N*H*$_2$), 2.96 (t, ^3J(H,H) = 5.1 Hz, 6 H; Ar−O−C*H*$_2$), 3.41 (t, 6 H; Ar−O−CH$_2$C*H*$_2$NH$_2$), 6.45 (s, 1 H; C*H*), 7.17 (d, ^4J(H,H) = 2.4 Hz, 3 H; Ar-*H*), 7.31 (d, ^4J(H,H) = 2.4 Hz, 3 H; Ar *H*). ^{13}C NMR ($CDCl_3$): $\delta = 152.9$ (Ar), 144.6 (Ar), 141.9 (Ar), 137.4 (Ar), 127.2 (Ar), 122.4 (Ar), 74.4 (Ar−O−*C*H$_2$), 42.4 (Ar−O−CH$_2$*C*H$_2$), 37.8 (*C*−H), 35.6 (Ar−*C*(CH$_3$)$_3$). 34.5 (Ar−*C*(CH$_3$)$_3$), 31.4 (Ar−C(*C*H$_3$)$_3$), 31.4 (Ar−C(*C*H$_3$)$_3$). Anal. Calcd for $C_{49}H_{79}N_3O_3$: C, 77.62; H, 10.50; N, 5.54. Found: C, 77.48; H, 10.56; N, 5.39.

Preparation of Tris(3,5-*tert*-butyl-2-(((diphenylphosphoryl)-acetamido)ethoxy)phenyl)methane, 8. A chloroform solution of **6** (8.00 g, 10.55 mmol) and *p*-nitrophenyl (diphenylphosphoryl)-acetate, **7** (12.50 g, 32.71 mmol), was stirred at 45 °C for 3 days. After cooling of the solution to room temperature, a 1 M solution of NaOH (100 mL) was added and the mixture was stirred for 2 h. The *p*-nitrophenol sodium salt was extracted from the chloroform solution using 5% sodium carbonate (6 × 300 mL), and the organic layer was further extracted with brine. The organic phase was dried with $MgSO_4$ and filtered and the solvent removed in vacuo to give an off-white solid material. The crude material was recrystallized from acetonitrile to give 14.84 g (95%) of crystalline product. IR: $\nu = 1670$ cm^{-1} (C═O), 1189 cm^{-1} (P═O). ^{1}H NMR (CD_3CN): $\delta = 1.12$ (s, 27 H; Ar−C(C*H*$_3$)$_3$), 1.30 (s, 27 H; Ar−C(C*H*$_3$)$_3$), 3.47 (d, J(H,P) = 13.5 Hz, 6H; C*H*$_2$–POAr$_2$), 3.49 (m, 6H; Ar−O−CH$_2$C*H*$_2$), 3.65 (t, ^3J(H,H) = 5.2 Hz, 6 H; Ar−O−C*H*$_2$), 6.28 (s, 1 H; C−*H*), 6.82 (d, ^4J(H,H) = 2.5 Hz, 3 H; Ar *H*), 7.25 (d, ^4J(H,H) = 2.5 Hz, 3 H; Ar *H*), 7.39 (m, 12 H; P−Ar *H*), 7.47 (m, 6 H; P−Ar *H*), 7.68 (m, 12 H; P−Ar *H*), 8.00 (t, ^3J(H,H) = 5.6 Hz, 3 H; N−*H*). ^{13}C NMR (CD_3CN): $\delta = 166.7$ (d, ^2J(C,P) = 5.5 Hz, C═O), 154.7 (Ar), 146.2 (Ar), 143.4 (Ar), 139.2 (Ar), 134.2 (d, J(C,P) = 105.7 Hz, P−Ar), 133.6 (Ar), 133.3 (P−Ar), 132.0 (d, J(C,P) = 9.6 Hz, P−Ar), 130.0 (d, J(C,P) = 12.1 Hz, P−Ar), 127.7 (Ar), 124.1 (Ar), 72.0 (Ar−O−*C*H$_2$), 40.9 (Ar−O−CH$_2$*C*H$_2$), 40.1 (*C*−H), 39.5 (d, J(C,P) = 63.4 Hz, *C*H$_2$POAr$_2$), 36.5 (Ar−*C*(CH$_3$)$_3$), 35.4 (Ar−*C*(CH$_3$)$_3$), 32.2 (Ar−C(*C*H$_3$)$_3$, 32.0 (Ar−C(*C*H$_3$)$_3$. ^{31}P NMR (CD_3CN): $\delta = 28.7$. ^{1}H NMR ($CDCl_3$): $\delta = 1.16$ (s, 27 H; Ar−C(C*H*$_3$)$_3$), 1.27 (s, 27 H; Ar−C(C*H*$_3$)$_3$), 3.44 (d, J(H,P) = 13.7 Hz, 6H; C*H*$_2$–POAr$_2$), 3.46 (m, 6H; Ar−O−CH$_2$C*H*$_2$), 3.46 (b, 6 H; Ar−O−C*H*$_2$), 6.35 (s, 1 H, C−*H*), 7.12 (b, 6 H; Ar *H*), 7.37 (m, 18 H; P−Ar *H*), 7.76 (m, 12 H; P−Ar *H*), 8.00 (t, ^3J(H,H) = 5.6 Hz, 3 H; N−*H*). ^{13}C NMR ($CDCl_3$): $\delta = 165.4$ (C═O), 153.3 (Ar), 144.8 (Ar), 142.0 (Ar), 137.5 (Ar), 132.2 (d, J(C,P) = 112.5 Hz; P−Ar), 132.2 (P−Ar), 131.2 (d, J(C,P) = 9.8 Hz; P−Ar), 128.8 (d, J(C,P) = 12.1 Hz; P−Ar), 127.0 (Ar), 122.5 (Ar), 70.7 (Ar−O−*C*H$_2$), 40.5 (Ar−O−CH$_2$*C*H$_2$), 39.1 (d, J(C,P) = 62.6 Hz; *C*H$_2$-POAr$_2$), 38.4 (*C*−H), 35.6 (Ar−*C*(CH$_3$)$_3$), 34.6 (Ar-*C*(CH$_3$)$_3$), 31.6 (Ar−C(*C*H$_3$)$_3$, 31.6 (Ar−C(*C*H$_3$)$_3$). ^{31}P NMR ($CDCl_3$): $\delta = 28.9$. Anal. Calcd for $C_{91}H_{112}N_3O_9P_3$: C, 73.61; H, 7.60; N, 2.83. Found: C, 73.44; H, 7.64; N, 2.73. Slow diffusion of pentane into a saturated solution of **8** in chloroform afforded crystals suitable for X-ray analysis.

Preparation of Metal Complexes. Preparation of [8·Th(NO$_3$)$_2$]-(NO$_3$)$_2$, 9. A solution of $Th(NO_3)_4 \cdot 4H_2O$ (0.025 g, 0.046 mmol) in 1 mL of methanol was added to a solution of **8** (0.068 g, 0.046 mmol) in 1 mL of methanol, and the mixture was stirred for 10 min. A white precipitate formed within minutes, and the product was collected by filtration, washed with cold methanol and ether, and dried to afford 0.088 g of product. Yield: 98%. IR: $\nu = 1617$ cm^{-1} (C═O), 1523 (N−O), 1289 (N−O), 1127 (P═O), 742 (N−O). ^{1}H NMR[CD_3CN:CD_3OD(1:1)]: $\delta = 1.15$ (s, 27 H; Ar−C(C*H*$_3$)$_3$), 1.19 (s, 27 H; Ar−C(C*H*$_3$)$_3$), 1.22 (m, 6H), 2.46 (d,

J(H,P) = 13.5 Hz, 2H; CH_2–POAr$_2$), 3.06 (d, J(H,P) = 8.2 Hz, 2H; CH_2–POAr$_2$), 3.52 (t, ^3J(H,H) = 7.1 Hz, 2H), 4.42 (t, ^3J(H,H) = 12.0 Hz, 2H), 6.31 (s, 1 H; C−*H*), 7.19 (d, ^4J(H,H) = 2.4 Hz, 3 H; Ar *H*), 7.43 (d, ^4J(H,H) = 2.4 Hz, 3 H; Ar *H*), 7.46 (b, 6 H; P−Ar *H*), 7.55 (b, 12 H; P−Ar *H*), 7.60 (b, 6 H; P−Ar *H*), 7.88 (b, 6 H; P−Ar *H*), 9.51 (b, 1 H (exchanges with solvent); N−*H*). ^{31}P NMR (CD$_3$CN): δ = 39.7. HR ESI-ICR MS (sample injected as solution in 1% HNO$_3$/MeOH): *m*/*z* 919.88, [**8**·Th(NO$_3$)$_2$]$^{2+}$. Anal. Calcd for $C_{91}H_{118}N_7O_{24}P_3Th$: C, 54.14; H, 5.89; N, 4.86. Found: C, 54.19; H, 5.71; N, 4.92. Slow diffusion of ether into a saturated acetone/methanol (1:1) solution of [**8**·Th(NO$_3$)$_2$](NO$_3$)$_2$ afforded crystals suitable for structural analysis.

General Procedure for the Preparation of [8·LnNO$_3$]Ln(NO$_3$)$_5$ (Ln = La, Ce, Nd, Eu, Yb). A solution of 2 equiv of Ln(NO$_3$)$_3$·*x*H$_2$O in CH$_3$CN was added to a solution of 1 equiv of **8** in CH$_3$CN. Within 5 min a precipitate formed, and the solid was collected, washed with cold acetonitrile and ether, and dried to afford product typically in yields ranging from 45% to 75%. Single isostructural crystals of the compounds could often be grown from saturated acetonitrile solutions, and although the crystals were of poor quality, a full structural determination of the Nd species was undertaken. In the solid state, two inequivalent lanthanides are coordinated by **8**, one of which contains an additional water ligand. This water molecule (0.5/complex) has been included in the calculated formula for the elemental analysis data. Crystalline material was also often obtained from saturated methanol solutions, but these tiny needlelike crystals were unsuitable for X-ray diffraction experiments. In the case of the Eu complex, elemental analysis (C, H, N, and P) of this material was consistent with the formulation [**8**·EuNO$_3$(H$_2$O)](NO$_3$)$_2$.

[8·LaNO$_3$]La(NO$_3$)$_5$, 10. Yield: 57%. IR: ν = 1629 cm^{-1} (C═O), 1459 (N−O), 1320 (N−O), 1161 (P═O), 735 (N−O). ^{1}H NMR (CD$_3$CN): δ = 1.16 (s, 27 H; Ar−C(CH_3)$_3$), 1.19 (s, 27 H; Ar−C(CH_3)$_3$), 3.60 (b, 6H; CH_2–POAr$_2$), 3.60 (b, 6H; Ar−O−CH_2CH_2), 3.60 (b, 6 H; Ar−O−CH_2), 6.31 (s, 1 H; C−*H*), 7.21 (d, ^4J(H,H) = 2.2 Hz, 3 H; Ar *H*), 7.37 (d, ^4J(H,H) = 2.2 Hz, 3 H; Ar *H*), 7.44 (m, 12 H; P−Ar *H*), 7.58 (m, 6 H; P−Ar *H*), 7.72 (b, 12 H; P−Ar *H*), 8.25 (b, 3 H; N−*H*). ^{31}P NMR (CD$_3$CN): δ = 36.1. HR ESI-ICR MS (sample injected as solution in 1% HNO$_3$/MeOH): *m*/*z* 842.33, [**8**·LaNO$_3$]$^{2+}$. Anal. Calcd for $C_{91}H_{113}N_9La_2O_{27.5}P_3$: C, 50.99; H, 5.31; N, 5.88. Found: C, 50.51; H, 5.23; N, 6.08.

[8·CeNO$_3$]Ce(NO$_3$)$_5$, 11. Yield: 60%. IR: ν = 1629 cm^{-1} (C═O), 1459 (N−O), 1320 (N−O), 1161 (P═O), 735 (N−O). ^{1}H NMR (CD$_3$CN): δ = 0.75 (s, 27 H; Ar−C(CH_3)$_3$), 0.89(s, 27 H; Ar−C(CH_3)$_3$), 3.80 (s, 1 H; C−*H*), 6.72 (d, ^4J(H,H) = 2.4 Hz, 3 H; Ar *H*), 6.84 (d, ^4J(H,H) = 2.4 Hz, 3 H; Ar *H*), 8.08 (b, 15 H), 9.92 (b, 12 H). ^{31}P NMR (CD$_3$CN): δ = 51.4 (broad). HR ESI-ICR MS (sample injected as solution in 1% HNO$_3$/MeOH): *m*/*z* 842.83, [**8**·CeNO$_3$]$^{2+}$. Anal. Calcd for $C_{91}H_{113}N_9Ce_2O_{27.5}P_3$: C, 50.93; H, 5.31; N, 5.87. Found: C, 51.06; H, 5.37; N, 5.69.

[8·NdNO$_3$]Nd(NO$_3$)$_5$, 12. Yield: 71%. IR: ν = 1629 cm^{-1} (C═O), 1477 (N−O), 1314 (N−O), 1161 (P═O), 737 (N−O). ^{1}H NMR (CD$_3$CN): δ = 0.70 (s, 27 H; Ar−C(CH_3)$_3$), 0.92 (s, 27 H; Ar−C(CH_3)$_3$), 6.74 (s, 3 H; Ar *H*), 6.84 (s, 3 H; Ar *H*), 7.89 (s, 1H; C−*H*), 8.18 (b, 12 H; P−Ar *H*), 9.60 (b, 6 H; P−Ar *H*), 10.20 (b, 12 H; P−Ar *H*). ^{31}P NMR (CD$_3$CN): δ = 67.7 (broad). HR ESI-ICR MS (sample injected as solution in 1% HNO$_3$/MeOH): *m*/*z* 843.83, [**8**·NdNO$_3$]$^{2+}$. Anal. Calcd for $C_{91}H_{113}N_9Nd_2O_{27.5}P_3$: C, 50.73; H, 5.29; N, 5.85. Found: C, 50.86; H, 5.26; N, 5.76.

[8·EuNO$_3$]Eu(NO$_3$)$_5$, 13. Yield: 45%. IR: ν = 1629 cm^{-1} (C═O), 1473 (N−O), 1307 (N−O), 1163 (P═O), 736 (N−O). ^{1}H NMR (CD$_3$CN): δ = 1.42 (s, 27 H; Ar−C(CH_3)$_3$), 1.60 (s, 27 H; Ar−C(CH_3)$_3$), 4.40 (b, 6 H; Ar−O−CH_2), 5.34 (b, 6H; Ar−O−CH$_2$CH_2), 6.75 (b, 12 H; P−Ar *H*), 7.11 (b, 12 H; P−Ar *H*), 7.56 (d, ^4J(H,H) = 2.4 Hz, 3 H; Ar *H*), 7.97 (d, ^4J(H,H) = 2.4 Hz, 3 H; Ar *H*), 8.64 (s, 1H; C−*H*), too broad to see N−*H*. ^{31}P NMR (CD$_3$CN): δ = −12.3 (broad). HR ESI-ICR MS (sample injected as solution in 1% HNO$_3$/MeOH): *m*/*z* 848.34, [**8**·EuNO$_3$]$^{2+}$. Anal. Calcd for $C_{91}H_{112}N_6O_{18}P_3Eu(H_2O)$: C, 59.38; H, 6.24; N, 4.57; P, 5.05. Found: C, 59.29; H, 6.24; N, 4.48; P, 4.88.

[8·YbNO$_3$]Yb(NO$_3$)$_5$, 14. Yield: 75%. IR: ν = 1628 cm^{-1} (C═O), 1481 (N−O), 1309 (N−O), 1162 (P═O), 737 (N−O). ^{1}H NMR (CD$_3$CN): δ = 1.68 (s, 27 H; Ar−C(CH_3)$_3$), 2.23 (s, 27 H; Ar−C(CH_3)$_3$), 5.02 (b), 6.16 (b), 7.95 (s, 3 H; Ar *H*), 8.55 (s, 3 H; Ar *H*), 10.81 (s, 1 H; C−*H*). ^{31}P NMR (CD$_3$CN): δ = 3.9 (broad). HR ESI-ICR MS (sample injected as solution in 1% HNO$_3$/MeOH): *m*/*z* 858.84, [**8**·YbNO$_3$]$^{2+}$. Anal. Calcd for $C_{91}H_{113}N_9O_{27.5}P_3Yb_2$: C, 49.41; H, 5.15; N, 5.70. Found: C, 50.24; H, 5.42; N, 5.38.

Preparation of 8·LiOC$_6$H$_2$N$_3$O$_6$, 15. *Warning! Picrate salts are potentially explosive and should be handled with great care*. A 0.013 g (0.05 mmol) portion of lithium picrate was added to a solution of 0.080 g (0.05 mmol) of **8** in 2 mL of chloroform. The reaction mixture was stirred at room temperature for 1 h to allow the lithium picrate to dissolve. The solvent was removed in vacuo and the residue washed with pentane to give 0.091 g of product. Yield: 98%. IR: ν = 1630 cm^{-1} (C═O), 1185 (P═O). ^{1}H NMR (CDCl$_3$): δ = 1.18 (s, 27 H; Ar−C(CH_3)$_3$), 1.19 (s, 27 H; Ar−C(CH_3)$_3$), 2.97 (d, J(H,P) = 8.1 Hz, 2H; CH_2–POAr$_2$), 3.21 (d, J(H,P) = 8.1 Hz, 2H; CH_2–POAr$_2$), 3.37 (t, 6H, ^3J(H,H) = 15.1 Hz; Ar−O−CH_2CH$_2$), 3.82 (m, 6 H; Ar−O−CH_2CH$_2$), 4.18 (b, 2 H; CH_2–POAr$_2$), 6.54 (s, 1 H; C−*H*), 7.10 (d, ^4J(H,H) = 2.4 Hz, 3 H; Ar *H*), 7.34 (d, ^4J(H,H) = 2.4 Hz, 3 H; Ar *H*), 7.45 (m, 18 H; P−Ar *H*), 7.80 (m, 12 H; P−Ar *H*), 8.34 (b, 3 H; N−*H*), 8.86 (s, 2 H; picrate). ^{13}C NMR (CDCl$_3$): δ = 181.0 (C═O), 166.0 (picrate), 162.2 (picrate), 153.0 (Ar), 145.0 (Ar), 142.1 (Ar), 141.8 (picrate), 137.2 (Ar), 132.8 (P−Ar), 131.2 (d, J(C,P) = 10.6 Hz, P−Ar), 130.9 (P−Ar), 129.2 (d, J(C,P) = 12.1 Hz, P−Ar), 128.9 (d, J(C,P) = 12.1 Hz, P−Ar), 126.8 (Ar), 122.9 (Ar), 69.9 (Ar−O−*C*H$_2$), 41.5 (Ar−O−CH$_2$*C*H$_2$), 38.6 (d, J(C,P) = 61.1 Hz, *C*H$_2$-POAr$_2$), 36.6 (*C*−H), 35.6 (Ar−*C*(CH$_3$)$_3$), 34.7 (Ar−*C*(CH$_3$)$_3$), 32.0 (Ar−C(*C*H$_3$)$_3$, 31.7(Ar−C(*C*H$_3$)$_3$. ^{31}P NMR (CDCl$_3$): δ = 32.6. Anal. Calcd for $C_{97}H_{114}LiN_6O_{16}P_3$: C, 67.74; H, 6.68; N, 4.89; Found: C, 67.71; H, 6.67; N, 4.93. Slow diffusion of pentane into a saturated solution of **8**·LiOC$_6$H$_2$N$_3$O$_6$ in chloroform produced crystals suitable for X-ray structural analysis.

X-ray Crystallography. Unit cell dimensions and intensity data for all the structures were obtained on a Siemens CCD SMART diffractometer at 173 K, with the exception of [**8**·Th(NO$_3$)$_2$](NO$_3$)$_2$, which was collected at 193 K. The data collections nominally covered over a hemisphere of reciprocal space, by a combination of three sets of exposures; each set had a different ϕ angle for the crystal, and each exposure covered 0.3° in ω. The crystal to detector distance was 5.0 cm. The data sets were corrected for absorption by using SADABS[16] or by measurement of crystal faces.

All the structures were solved using the Bruker SHELXTL software package for the PC, using either direct methods or Patterson functions in SHELXS. The space groups of the compounds were determined from an examination of the systematic absences in the data, and the successful solution and refinement of the structures confirmed these assignments. All hydrogen atoms were assigned idealized locations and were given a thermal parameter equivalent to 1.2 or 1.5 times the thermal parameter of

(16) Blessing, R. H. *Acta Crystallogr., Sect. A* 1995, *51*, 33.

Table 1. X-ray Data[a] for the Crystal Structures of **8** and the Complexes **9**, **12**, and **15**

	8·C_5H_{12}	**9**·2.5MeOH·0.5Et_2O	(**12a,b**)·7.25CH_3CN	**15**·4$CHCl_3$
tot. reflcns	45 472	25 051	45 369	28 811
unique reflcns	15 253	16 050	27 965	18 059
θ_{max} (deg)	24.72	24.00	22.50	24.50
empirical formula	$C_{96}H_{124}N_3O_9P_3$	$C_{95.5}H_{122}N_7O_{24}P_3Th$	$C_{198}H_{250}N_{26}Nd_4O_{55}P_6$	$C_{101}H_{118}Cl_{12}LiN_6O_{16}P_3$
M_r	1556.89	2076.95	4637.11	2197.26
cryst system	monoclinic	triclinic	triclinic	triclinic
space group	$P2_1/c$	$P\bar{1}$	$P\bar{1}$	$P\bar{1}$
a (Å)	18.207(2)	12.3375(8)	14.4930(7)	12.091(1)
b (Å)	22.309(3)	17.742(1)	23.024(1)	16.743(2)
c (Å)	22.805(3)	24.853(2)	34.534(2)	28.071(3)
α (deg)		102.478(1)	80.964(1)	102.015(2)
β (deg)	105.212(5)	102.155(1)	81.605(1)	91.830(2)
γ (deg)		95.590(1)	86.256(1)	100.091(2)
V_c (Å^3)	8938(2)	5134.0(6)	11 248(1)	5458.0(8)
D_c (g cm^{-3})	1.157	1.344	1.348	1.337
Z	4	2	2	2
μ(Mo Kα) (mm^{-1})	0.124	1.571	1.030	0.412
R_1 [$I \geq 2\sigma(I)$ data][b]	0.0544 [10 611]	0.0706 [9115]	0.0961 [14 290]	0.0798 [8877]
wR_2 (all data)[c]	0.1450	0.1624	0.2531	0.2073
GoF	1.089	0.954	0.986	0.962
larg diff peak, hole (e Å^{-3})	+0.39, 0.31	+1.00, 1.29	+1.51, 1.56	+0.63, 0.46

[a] Obtained with monochromatic Mo K radiation (λ = 0.710 73 Å) at 173 K for **8**, **12**, and **15** and 193 K for **9**. [b] $R_1 = \Sigma||F_o| - |F_c||/\Sigma F_o$. [c] $wR_2 = \{\Sigma[w(F_o^2 - F_c^2)^2/\Sigma[w(F_o^2)^2]\}^{1/2}$.

Table 2. Selected Bond Lengths (Å) for the Compounds **8**, **9**, **12a,b**, and **15**

	8	**9,** M = Th(1)	**12a**, M = Nd(1′)	**12b**, M = Nd(1)	**15,** M = Li(1)
P(1)−O(5)	1.4833(19)	1.516(7)	1.472(9)	1.486(10)	1.503(3)
P(2)−O(7)	1.487(2)	1.511(6)	1.490(10)	1.519(9)	1.494(3)
P(3)−O(9)	1.4872(18)	1.485(7)	1.484(10)	1.510(9)	1.481(3)
C(46)−O(4)	1.225(3)	1.276(11)	1.219(16)	1.240(16)	1.228(6)
C(62)−O(6)	1.236(3)	1.233(10)	1.261(17)	1.252(16)	1.252(6)
C(78)−O(8)	1.230(3)	1.262(11)	1.214(15)	1.236(14)	1.238(6)
M−O(5)		2.431(6)	2.434(9)	2.405(8)	1.942(9)
M−O(7)		2.395(6)	2.436(10)	2.394(9)	1.935(9)
M−O(9)		2.412(7)	2.429(9)	2.452(9)	1.863(9)
M−O(4)		2.419(6)	2.482(9)	2.358(9)	
M−O(6)		2.483(6)	2.430(10)	2.386(9)	2.005(8)
M−O(8)		2.419(6)	2.490(10)	2.437(9)	
M−O(10)		2.664(7)	2.615(10)	2.535(10)	
M−O(11)		2.528(6)	2.621(10)	2.552(10)	
M−O(13)		2.613(8)			
M−O(14)		2.637(8)			
M−O(100)			2.518(10)		

the atom to which it was attached. For the methyl groups, where the location of the hydrogen atoms is uncertain, the AFIX 137 card was used to allow the hydrogen atoms to rotate to the maximum area of residual density, while fixing their geometry. In cases of extreme disorder or other problems, the non-hydrogen atoms were refined only isotropically, and hydrogen atoms were not included in the model. Severely disordered solvents were removed from the data for **8**, **9**, **12**, and **15** using the SQUEEZE function in the Platon for Windows software[17] and the details reported in the Supporting Information in the CIF file for each structure. Structural and refinement data and selected bond lengths for all the compounds are presented in Tables 1 and 2.

Results and Discussion

To develop a functional tris-CMPO ligand system, three CMPO groups can be attached to a platform capable of preorganizing these moieties for cooperative metal binding. Previous work with the triphenoxymethane platform, **4**, has shown that when all three phenol oxygens on **4** are substituted, the conformation with these oxygen atoms "all up" (Figure 1) relative to the central methine hydrogen of the platform exclusively exists both in the solid state and in solution.[15] Tethering three CMPO moieties to this platform via these phenol oxygens satisfies the requirement for proximate metal binding CMPO groups while the six *tert*-butyl groups at the periphery increase the solubility of the final ligand product and its metal complexes in organic solvents. As outlined in Scheme 1, the synthesis of the tris-CMPO ligand follows the well-established derivatization methods of the CMPO−calixarene systems.[10] Since all steps

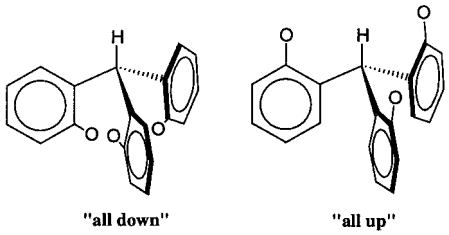

Figure 1. Illustration of the two extreme conformations of the oxygen atoms on the triphenoxymethane platform relative to its central methine hydrogen.

(17) van der Sluis, P.; Spek, A. L. *Acta Cryst.* **1990**, *A46*, 194.

Scheme 1 [a]

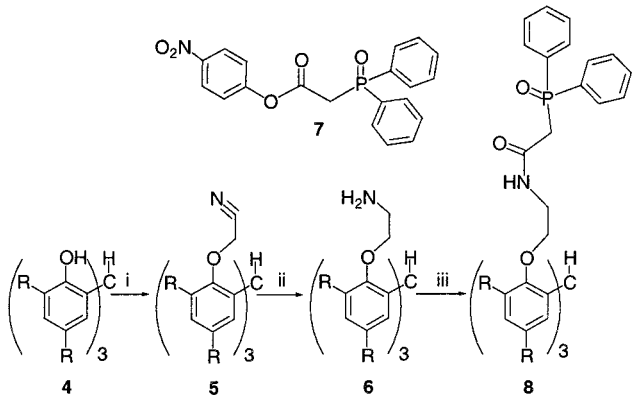

[a] Key: (i) K_2CO_3, NaI, $ClCH_2CN$, refluxing acetone, 2 days, 75%; (ii) $LiAlH_4$, Et_2O, rt overnight, 70%; (iii) **7**, $CHCl_3$, 45 °C, 3 days, 95%. Note: R = *t*-Bu.

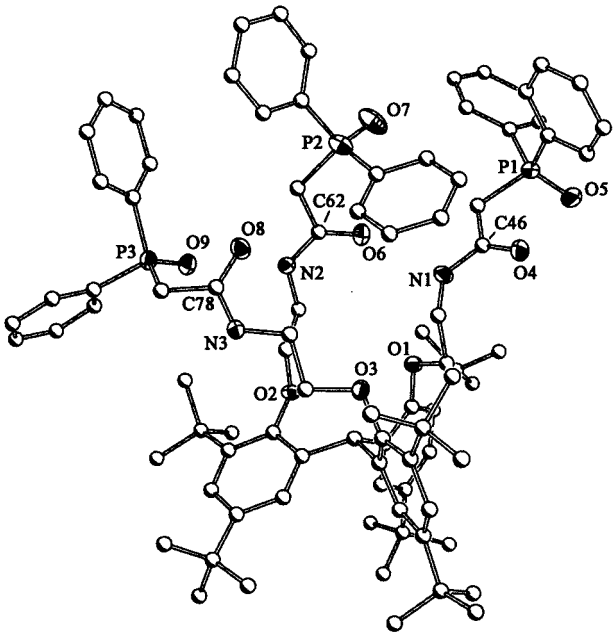

Figure 2. Diagram of the structure of **8** (40% probability ellipsoids for N, O, and P atoms; carbon atoms drawn with arbitrary radii). All hydrogen atoms have been omitted for clarity.

in this synthesis are high yielding, multigram quantities of the ligand can be produced with little synthetic effort. X-ray crystal structures of the intermediate product, **5** (see Supporting Information), and the tris-CMPO ligand, **8** (Figure 2), illustrate that, indeed, the conformation of the platform is "all up" and that the three CMPO moieties in **8** are poised for cooperative metal binding. Moreover, with the three arms situated in such close proximity, large metal ions capable of interacting with the ligand will be simultaneously bound by all three arms of **8**, each in a bidentate fashion.

The conditions of the actinide and lanthanide extraction experiments were chosen both to mimic the acidic environment of the TRUEX process and to allow a direct comparison between the extraction properties of **8** and other published multiple-CMPO ligand systems such as **2** and **3**. Initially, 10^{-4} M solutions of the nitrate salts of the lanthanides, lanthanum, cerium, neodymium, europium, and ytterbium, and the actinides, thorium and uranyl, in 1 M nitric acid were

Table 3. Extraction Percentage (% *E*)[a] for **1**−**3** and **8**

cation (10^{-4} M) in 1 M HNO_3	equiv of ligand in organic phase[b]	**8** (% *E*)	**1**[c] (% *E*)	**2**[d] (% *E*)	**3**[d] (% *E*)
Th^{4+}	1	40 ± 1		76 ± 1	61 ± 1
	10	98 ± 1		>90	> 90
	100		12.2		
UO_2^{2+}	10	45 ± 1			
La^{3+}	10	4 ± 1		19 ± 1	98 ± 1
	50	9 ± 1			
Ce^{3+}	10	5 ± 1			
	50	13 ± 1			
Nd^{3+}	10	3 ± 1			
	50	15 ± 1			
Eu^{3+}	10	3 ± 1		16 ± 1	58 ± 1
	50	10 ± 1		63 ± 3	
	2500		69.5		
Yb^{3+}	10	10 ± 1		2.6 ± 0.7	3 ± 1
	50	12 ± 1			
Th^{4+}(mixed)[e]	10	98 ± 1			
UO_2^{2+}(mixed)[e]		41 ± 1			
La^{3+}(mixed)[e]		3 ± 1			
Eu^{3+}(mixed)[e]		2 ± 1			

[a] % $E = 100\%([M^{n+}]_{org}/[M^{n+}]_{tot.})$ after extraction as determined by Arsenazo(III) assay. [b] In a volume of CH_2Cl_2 equal to the volume of the aqueous phase. [c] Data reported from ref 8. [d] Data reported from ref 10. [e] Extraction percentages for a single solution containing Th^{4+}, UO_2^{2+}, La^{3+}, and Eu^{3+} (each 10^{-4} M), determined by ICP-MS.

extracted with an equal volume of a 10^{-3} M methylene chloride solution of **8**. Due to the quantitative removal of thorium from the aqueous phase under these initial conditions, the extraction experiment for this metal was repeated using a 10^{-4} M solution of **8** in methylene chloride to obtain a reportable extraction percentage; however, the quantitative extraction of thorium under the lanthanide extraction conditions will be discussed herein to prevent confusion. Experiments using two different ligand concentrations resulted in the extraction of the thorium metal as a suspension. A competition experiment using a mixed metal aqueous phase containing 10^{-4} M each of lanthanum, europium, thorium, and uranyl nitrate in 1 M nitric acid and a 10^{-3} M methylene chloride solution of **8** in the organic phase was also performed. The extractability of the metal ion in all cases was determined by measuring the metal concentration in the nitric acid phase before and after the extraction with solutions of **8**. These extraction results are presented with the results of the most fully studied of the tetra-CMPO calixarene systems, **2** and **3**, in Table 3 and Chart 1.

The results of the extraction experiments reveal that **8** has a high affinity for actinides similar in magnitude to the CMPO−calixarene systems, but unlike these other systems, **8** has a low and constant affinity for lanthanides across the series. Initially, the selectivity of **8** for actinides was attributed to the strong cooperative binding potential among its closely spaced CMPO moieties and the ability of the ligand to mimic the 3:1 stoichiometry implicated in the TRUEX process, but lanthanides should form analogous species with **8** leading to their removal from the aqueous phase of the experiment. To gain an understanding of the differences between the actinide and lanthanide complexes generated during these extractions, complexes of **8** with lanthanide and actinide metals were synthesized and characterized. The fully hydrated nitrate salts of these metals were utilized in the preparation of these complexes to provide the exogenous

Chart 1. Metal Extraction Percentages (% *E*) for the Ligands **2**,[10] **3**,[10] and **8** Using 10^{-4} M Metal Nitrate in 1 M Nitric Acid and 10^{-3} M Ligand in Methylene Chloride[a]

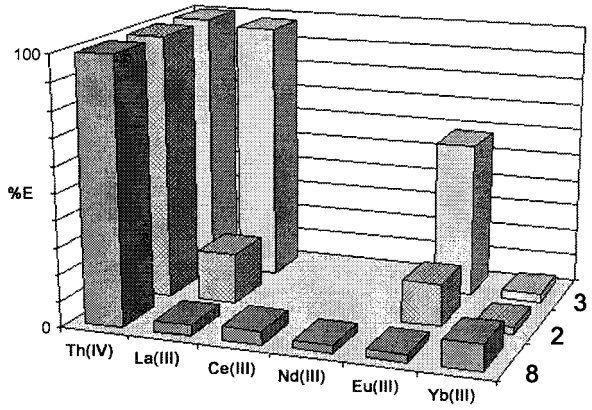

[a] The thorium extraction percentages for **2** and **3** at this ligand concentration were both reported as greater than 90%.[10]

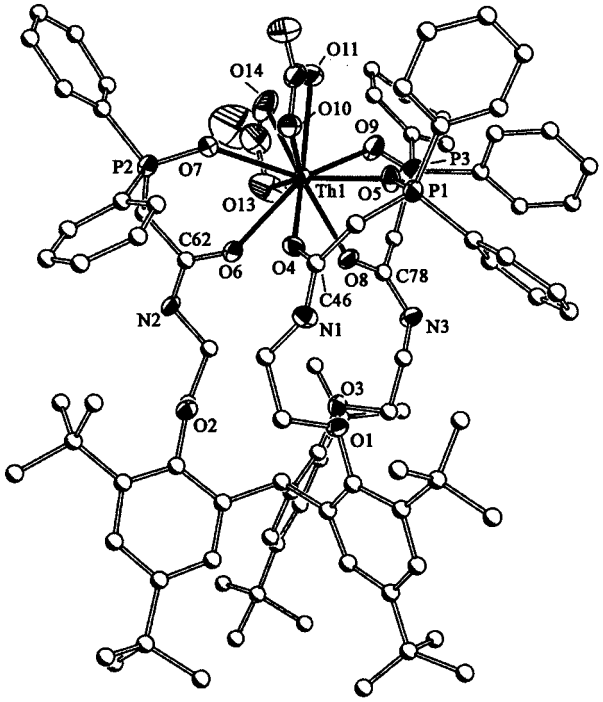

Figure 3. Diagram of the structure of **9** (40% probability ellipsoids for Th, N, O, and P atoms; carbon atoms drawn with arbitrary radii). All hydrogen atoms have been omitted and the thorium−ligand bonds have been drawn with solid lines.

water ligands and nitrate counterions available to them when dissolved in 1 M nitric acid.

The crystal structure of the thorium nitrate complex of **8** is shown in Figure 3, and the cooperative binding of all three CMPO arms through their six oxygen donor atoms is readily apparent. The tight binding of the tetravalent metal by these three bulky ligand moieties allows space on the metal for only two of its four nitrate counterions and no coordinated water molecules, generating a 2+ cationic complex. To confirm the existence of this structure in solution and its relevance to the extracted material, the ^{1}H and ^{31}P NMR and the Fourier transform ion cyclotron resonance mass spectrometry (FT-ICR-MS) spectra of the complex were examined. The ^{31}P NMR spectrum of the mixture verified the

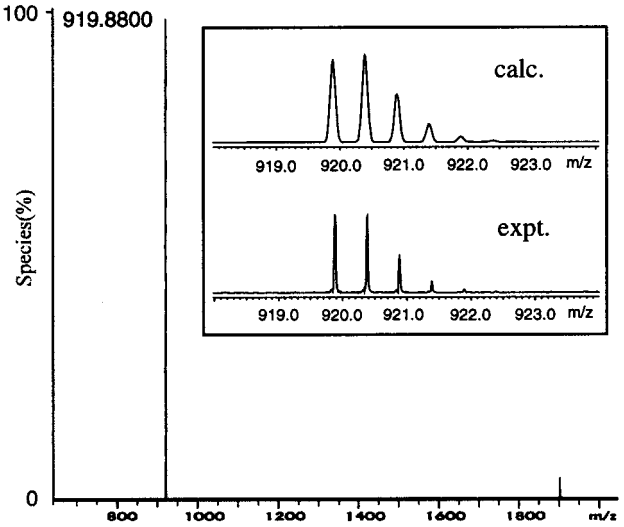

Figure 4. FT-ICR-MS spectrum of **9** demonstrating that the 2+ cationic complex exists in solution. The small peak at ~1900 corresponds to a 1+ complex containing an undissociated nitrate anion. The inset shows the theoretical and actual isotope distribution patterns of the 2+ cationic complex of **9**.

cooperative binding in solution of the thorium ion by all three CMPO moieties in **8**. The complex exhibits a single phosphorus resonance shifted 11 ppm downfield in comparison to the spectrum of the ligand, in agreement with all three CMPO moieties binding the metal simultaneously in solution. For the FT-ICR-MS spectrum, the complex was acidified with nitric acid prior to injection, and the spectrum (Figure 4) of this solution contains almost exclusively the 2+ cationic complex from the crystal structure. Finally, the arrangement in solution of the two coordinated nitrate counterions and the three coordinated CMPO groups, verified by FT-ICR-MS and ^{31}P NMR spectra, respectively, was shown to match the solid-state structure by ^{1}H NMR spectroscopy. The coordination of the thorium ion by the two nitrate counterions disrupts the C_3-symmetric environment induced by the ligand. In the ^{1}H NMR spectrum of the complex, resonances associated with analogous linker moiety hydrogens located near this asymmetry differentiate relative to the ^{1}H NMR spectrum of **8**, while resonances associated with the less affected triphenoxymethane portion of the complex retain their symmetry in solution (spectrum in Supporting Information). The solubility of this complex in methylene chloride is minimal, thus accounting for the suspension in the organic phase of the extraction experiments. Complexes of **8** with uranyl nitrate could not be isolated and characterized, but due to the linear arrangement of the two oxo groups on the metal ion, the structure of a uranyl nitrate complex with **8** must significantly differ from the thorium species. Efforts are in progress to characterize the structure of the uranyl complex and determine a basis for the affinity of **8** for uranyl ion.

The solid- and solution-state structures of the lanthanide complexes of **8** were similarly determined using X-ray crystallography, NMR, and mass spectrometry. An X-ray crystal structure of the neodymium complex was obtained, and the two slightly different neodymium complexes found in the asymmetric unit are shown in Figures 5 and 6. Both

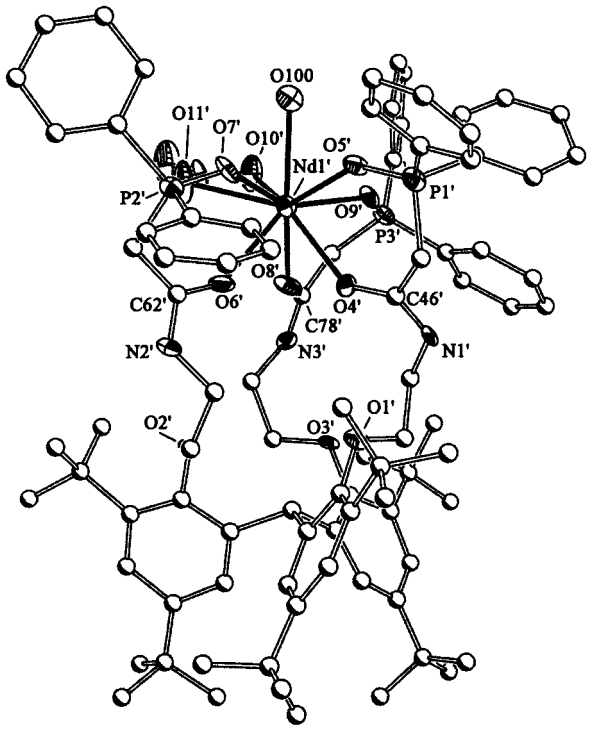

Figure 5. Diagram of the structure of **12a** (40% probability ellipsoids for Nd, N, O, and P atoms; carbon atoms drawn with arbitrary radii). For clarity, the neodymium−ligand bonds have been drawn with solid lines and all hydrogen atoms omitted.

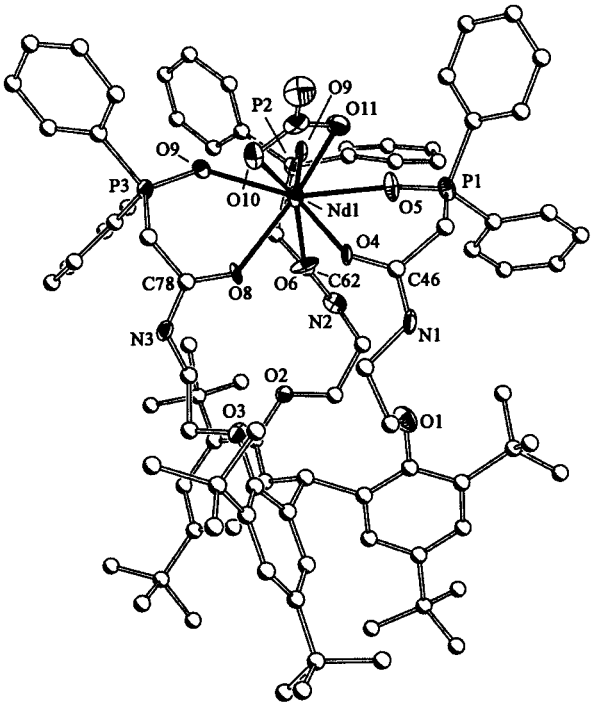

Figure 6. Diagram of the structure of **12b** (40% probability ellipsoids for Nd, N, O, and P atoms; carbon atoms drawn with arbitrary radii). The neodymium−ligand bonds have been drawn with solid lines and all hydrogen atoms omitted for clarity.

of these complexes contain a neodymium ion fully coordinated by the three CMPO moieties from **8** and a single bidentate nitrate counterion. The 2+ charge of each of these symmetry inequivalent complexes is balanced by a $Nd(NO_3)_5^{2-}$ counterion. In one of the neodymium complexes of **8**, **12a**,

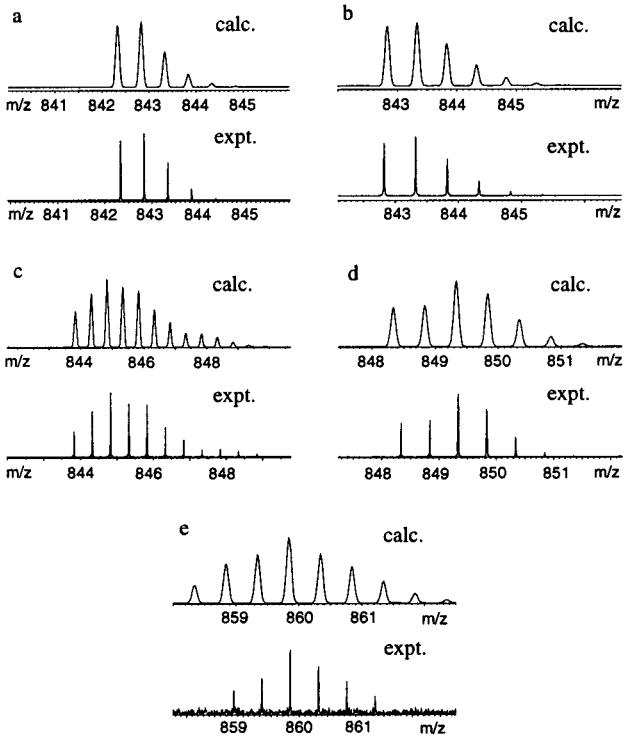

Figure 7. Theoretical and actual isotope distribution patterns of the 2+ cationic complex of (a) **10**, (b) **11**, (c) **12**, (d) **13**, and (e) **14** from their FT-ICR-MS spectra.

the metal is coordinated by a water molecule while the neodymium in the other complex with **8**, **12b**, is anhydrous, demonstrating the flexibility of the coordination environment around the metal. Nevertheless, in each case, there does not appear to be enough space to accommodate a second coordinated nitrate counterion. In both **12a,b**, the three CMPO arms of **8** have wrapped around the metal ion and bind in a bidentate fashion. The Nd−O distances in both complexes are marginally shorter than the bis-CMPO−Nd complex, $[(Ph_2P(O)CH_2C(O)NEt_2)_2Nd(NO_3)_3]$, characterized by Paine and co-workers,[6a] consistent with the decrease in coordination numbers of the metals.

Crystals of the europium complex of **8** were also obtained and were determined to be isostructural to the neodymium complex by unit cell determination. The existence of the anhydrous 2+ cationic neodymium complex in solution was confirmed by FT-ICR-MS using the same acidic sample preparation condition used for the thorium complex (Figure 7). The ^{31}P NMR spectrum of the complex shows a single shifted resonance consistent with all three CMPO moieties coordinating to the metal, but the peak is broadened and the shift is larger in magnitude relative to the corresponding peak in the ^{31}P NMR spectrum of the thorium complex due to paramagnetic effects from the trivalent neodymium ion. Because of this paramagnetism, peaks in the ^1H NMR spectrum of the neodymium complex were too broadened to determine structural features of the complex in solution; however, the ^1H NMR spectrum of the diamagnetic lanthanum nitrate complex of **8** reveals shifted proton resonances and a preservation of the C_3 symmetry of the complex. The lack of induced asymmetry from the coordinated nitrate

counterion in the spectrum is most likely due to the flexibility of the coordination environment around the metal apparent from the crystal structure of the neodymium complex. The lanthanum, cerium, europium, and ytterbium nitrate complexes of **8** were also characterized by ^{31}P NMR and FT-ICR-MS, and given the similarities in spectroscopic and extraction properties these compounds share with neodymium, it seems likely that extracted species of these metals exist in solution as anhydrous 2+ cationic complexes fully coordinated by all three CMPO moieties from the ligand (Figure 7). As noted above with the thorium complex, these lanthanide complexes of **8** are insoluble in methylene chloride.

The characterization of the thorium and lanthanide complexes of **8** that are likely formed during the extraction experiments at first glance reveal few differences to account for the high thorium selectivity of **8** relative to its lanthanide selectivity. Upon complexation by **8**, all of the metal ions form 2+ cationic complexes. By tight coordination to the metals, the bulkiness of the tris-CMPO ligand essentially "equalizes" the physical properties of the actinide and lanthanide complexes. The compounds are all very similar in size and shape and exhibit identical solubility properties. Yet, in the acidic solutions, the thorium complex is extracted to a much greater extent. As suggested by Seaborg,[18] trivalent actinides and lanthanides can be separated using ion-chromatography columns due the ability of the actinide to employ 5f-hybrid orbitals in bonding, and this unique attribute may have some influence in the extraction of actinides with **8**. Additionally, since the thorium ion is tetravalent, the increased Lewis acidity relative to the trivalent lanthanide ions may favor its extraction with **8**. One or both of these effects could account for the quantitative extraction of thorium as a suspended complex of **8** under conditions which disfavor the formation of lanthanide complexes, and further experiments with **8**, particularly with trivalent actinides, are in progress to ascertain the basis for the selectivity of **8** toward thorium(IV) witnessed in these experiments.

Further demonstrating that selectivity based upon small differences in the stability of the extracted metal complexes is possible, an enhanced extraction of the smallest ion was noted when aqueous alkali-metal picrate solutions were mixed with chloroform solutions of **8**. Aqueous lithium, sodium, potassium, rubidium, and cesium picrate solutions were extracted by equimolar amounts of chloroform solutions of **8**, and the results are reported in Chart 2. Attempts to synthesize and characterize alkali-metal picrate complexes of **8** for a structural comparison analogous to the actinide/lanthanide work detailed above resulted solely in the formation of a stable complex with lithium. The sodium, potassium, rubidium, and cesium complexes could not be isolated, and ^{1}H and ^{31}P NMR spectra of equimolar mixtures of these picrate salts and **8** confirm that no interactions between these metals and the CMPO moieties on **8** exist. The lithium picrate complex of **8** was successfully isolated and characterized in the solid state by X-ray crystallography. The ^{1}H, ^{13}C, and ^{31}P NMR spectra of the complex clearly indicate that the structure of this complex in solution is equivalent to the solid-state structure. In the lithium complex as highlighted in Figure 8, all three CMPO moieties bind to lithium ion in a tetrahedral arrangement about the metal using three phosphoryl oxygens and one carbonyl oxygen. In the ^{31}P NMR spectrum of the complex, a single shifted resonance corresponding to the three coordinated phosphoryl groups from the ligand verifies that all three CMPO groups coordinate to the metal, while the asymmetry the tetrahedral coordination environment induces onto the C_3 symmetric environment of the ligand is evident in the ^{1}H NMR spectrum as illustrated in Figure 9. Using this structural information, the selectivity of lithium by **8** over the other alkali metals can be rationalized by two factors. The smaller lithium metal has a higher charge density in comparison to the other alkali metals, and this difference increases the strength of its

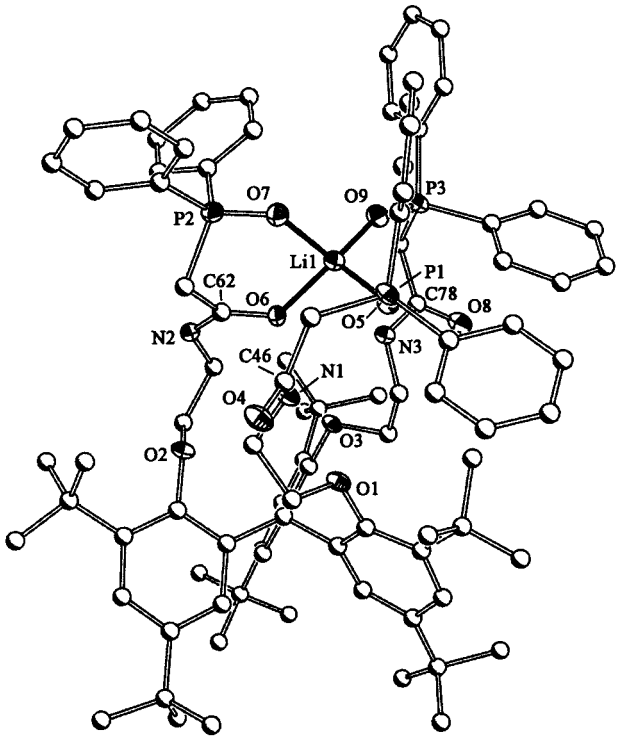

Figure 8. Diagram of the structure of **15** (40% probability ellipsoids for Li, N, O, and P atoms; carbon atoms drawn with arbitrary radii). Bonds to the lithium atom are indicated with solid lines. For clarity, all hydrogen atoms have been omitted.

Chart 2. Alkali-Metal Extraction Percentages (% *E*) for **8** Using Equimolar Amounts of Ligand in Chloroform and the Metal Picrate Salt in Water

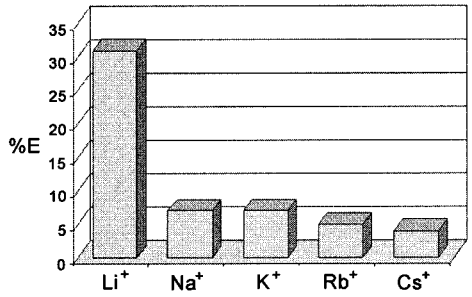

(18) Diamond, R. M.; Street, K.; Seaborg, G. T. *J. Am. Chem. Soc.* **1954**, *76*, 1461.

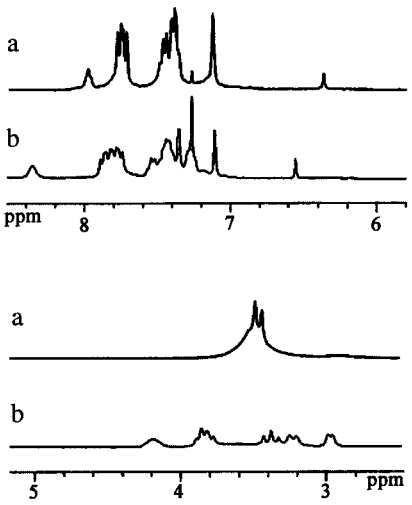

Figure 9. ^{1}H NMR spectra (in $CDCl_3$) of (a) **8** and (b) **15,** demonstrating the loss of C_3 symmetry upon coordination of the lithium ion. Note the shifts of the N−H peaks at (a) ∼7.9 and (b) ∼8.4 ppm and methine H peaks at (a) ∼6.4 and (b) ∼6.5 ppm and the differentiation of the three sets of CH_2 peaks between 3 and 4 ppm upon lithium complexation.

interactions with Lewis bases such as the oxygen donors on the CMPO moieties on **8**. The tetrahedral coordination geometry of the lithium ion is also perfectly accommodated by the donor atoms from **8**, especially by the bidentate coordination of one of the CMPO moieties, while the larger metals cannot adopt such a symmetric coordination environment with a single molecule of **8**. These small differences in Lewis acidity and coordination geometry are very likely responsible for the differences in selectivities that **8** exhibits for lithium over the other alkali metals.

Conclusions

Increasing the selectivity of ligand systems for actinides over lanthanides is essential for improving nuclear waste treatment processes, but unfortunately, the continued refinement of multi-CMPO-based extraction procedures has been hindered by problems associated with the characterization of the ligand−metal interactions involved in the extraction process. Taking inspiration from the suggested coordination environment of the extracted species in the TRUEX process, a C_3-symmteric tris-CMPO ligand system, **8**, was developed and shown to exhibit a higher selectivity for the actinide thorium over all of the lanthanides in comparison to other multi-CMPO systems such as **2** and **3**. The characterization of both the thorium and lanthanide complexes formed with **8** provides a possible explanation for the enhanced selectively of **8**. The three CMPO moieties on the ligand tightly coordinate both Th^{4+} and Ln^{3+}, leaving only enough space in the remaining metal coordination sphere to accommodate one or two nitrate counterions. Thus both Th^{4+} and Ln^{3+} form complexes with essentially the same shape and an equivalent 2+ charge. In view of this similarity in size and charge between the two complexes, the selectivity of **8** for thorium over the lanthanides may be attributed to the higher intrinsic stability of the thorium complex created by the combined effects of its increased Lewis acidity relative to the trivalent lanthanides and the increased ability of the actinide metal to accommodate the coordination environment presented by the ligand. Similar metal complex stability effects were shown to influence the alkali-metal extraction properties of **8**.

If actinide selectivity in this system is controlled by the charge density of the metal and its coordination geometry, small alterations can be made to the ligand system to exploit these differences and further increase its affinity for these metals. Accordingly, procedures to incorporate modifications that alter the basicity of the CMPO oxygen donors as well as the distance between adjacent CMPO groups on the triphenoxymethane platform are in progress. Future work will also involve the determination of the extraction behavior of **8** with trivalent actinides such as americium and the characterization of the complexes of these metals with **8**.

Acknowledgment. We thank the National Science Foundation (Grant CHE 9874966) and the donors of the American Chemical Society Petroleum Research Fund for funding this research. We are especially grateful to Prof. Benjamin A. Horenstein for the use of his radionuclide facility and to Drs. Lidia Matveeva and David H. Powell for their help with the FT-ICR-MS work.

Supporting Information Available: The NMR spectra of **8** and **9**, an ORTEP diagram for the X-ray crystal structure of **5**, and X-ray crystallographic files, in CIF format, for the structure determinations of **5**, **8**, and the complexes **9**, **12**, and **15**. This material is available free of charge via the Internet at http://pubs/acs.org.

IC011144X